Tellus
SERIES B
CHEMICAL
AND PHYSICAL
METEOROLOGY
PUBLISHED BY THE INTERNATIONAL METEOROLOGICAL INSTITUTE IN STOCKHOLM

*Tellus (2010), 62B, 595–607*

TELLUS

# Origin of $CO_2$ undersaturation in the western tropical Atlantic

*By* NATHALIE LEFÈVRE[1]*, DENIS DIVERRÈS[2] and FRANCIS GALLOIS[3], [1]*LOCEAN, Université P. et M. Curie, 4 place Jussieu, 75252 Paris Cedex 05, France;* [2]*US 191, Centre IRD de Bretagne, BP 70, 29280 Plouzané, France;* [3]*IRD Nouméa, 98848, Nouvelle Calédonie*

(Manuscript received 24 November 2009; in final form 3 June 2010)

ABSTRACT

Underway $fCO_2$ has been measured from two merchant ships sailing from France to French Guyana and France to Brazil, and during two zonal cruises from Africa to French Guyana. In the western Tropical Atlantic, the strongest undersaturation is associated with the Amazon discharge near 55°W. In the 5°S–10°N, 65–35°W region, the carbon system is strongly correlated to salinity and robust empirical relationships could be determined. This region is a sink of $CO_2$ in May–June during the high-flow period of the Amazon river. The eastward propagation of Amazon waters is observed when the retroflection of the North Brazil Current takes place. In August 2008, freshwater is observed as far as 40°W when the North Equatorial Counter Current is quite strong. The Amazon plume, defined as salinities less than 34.9, is a sink of $CO_2$ of 0.96 mmol $m^{-2}\,d^{-1}$. Further east, near 27°W, $CO_2$ undersaturation is recorded thoughout the year between 5°N and 8°N. This is caused by the high precipitation associated with the presence of the intertropical convergence zone (ITCZ). Removing the temperature effect leads to low (high) $fCO_2$ associated with low (high) salinities in boreal summer (winter), which is consistent with the seasonal migration of the ITCZ.

## 1. Introduction

The tropical Atlantic is a source of $CO_2$ for the atmosphere because of the equatorial upwelling supplying $CO_2$ rich waters to the surface. Waters from the equatorial upwelling supply $CO_2$ to the surface and the waters are transported westward by the South Equatorial Current (SEC). Andrié et al. (1986) showed that the fugacity of $CO_2$ in sea water ($fCO_2$) increases westward due to the warming of surface waters flowing from the African coast to the American coast between 15°S and 2°N. Oudot et al. (1987) reported high $fCO_2$ in this current.

Further north, lower sea surface salinities are observed in the North Equatorial Counter Current (NECC) that develops between approximately 2°N and 10°N. The climatology of Takahashi et al. (2009) shows an $fCO_2$ gradient between these two current systems with higher values south of 2°N and lower values in the NECC region but, on average, seawater $fCO_2$ is above the atmospheric level. This North–South gradient was also recently observed by Padin et al. (2009) who reported near-equilibrium conditions between 1°N and 8°N around 28°W during their FICARAM cruises while $CO_2$ supersaturation occurred further south between 1°N and 15°S. A few cruises have reported $CO_2$ concentrations below the atmospheric level in the north western tropical Atlantic and the origin of the $CO_2$ undersaturation was attributed to the discharge of the Amazon outflow (Ternon et al., 2000; Körtzinger, 2003). The Amazon is the largest river in the world representing about 20% of river supply to the world ocean, with a flow of 0.2 Sv (1 Sv $= 10^6$ $m^3$ $s^{-1}$). In the river, $fCO_2$ values over 4000 $\mu$atm have been reported, which is one order of magnitude higher than in the ocean, due to in situ respiration of organic carbon (Richey et al., 2002; Mayorga et al., 2005), making this river a strong source of $CO_2$. When Amazon waters mix with oceanic waters, the turbidity decreases and biological productivity can occur (Demaster et al., 1996). The very low DIC and $fCO_2$ values measured in the ocean correspond to the large $CO_2$ drawdown caused by strong biological activity but the high correlation observed with very low salinity (Ternon et al., 2000) confirms that this biological activity is due to the freshwater supply of the Amazon mixing with oceanic waters. This explains the ocean $CO_2$ sink reported near the Amazon outflow (e.g. Cooley et al., 2007). In addition to the Amazon outflow, the NECC region exhibits low salinities due to the presence of the Inter Tropical Convergence Zone (ITCZ) associated with high precipitation. This contributes to lower the fugacity of $CO_2$ north of the equator (Oudot et al., 1987). A strong correlation

*Corresponding author.
e-mail: nathalie.lefevre@locean-ipsl.upmc.fr
DOI: 10.1111/j.1600-0889.2010.00475.x

between $fCO_2$ and SSS has been observed for the western tropical Atlantic with a slope of 11 $\mu$atm psu$^{-1}$ (Ternon et al., 2000) and 13 $\mu$atm psu$^{-1}$ (Körtzinger, 2003) and for the equatorial band between 5°N and 5°S with a slope of 44 $\mu$atm psu$^{-1}$ (Oudot et al., 1995).

The occurrence and the extent of the low $CO_2$ concentrations area in the tropical Atlantic are not well documented. During fall, the retroflection of the North Brazil Current (NBC) can transport Amazon waters far east. As the equilibrium time of $CO_2$ with the atmosphere is quite slow, undersaturation area can persist far from the region where it is produced as observed during an Atlantic Meridional Transect made in October 1995 (Lefèvre et al., 1998). This might affect the $CO_2$ budget in the tropical Atlantic.

As part of the European project CARBOOCEAN, two merchant ships have been equipped with an autonomous $fCO_2$ system. $CO_2$ measurements have been collected on the merchant ships sailing from France to French Guyana and France to Brazil, providing repeated sampling of the Atlantic. In this paper, we focus on the western tropical Atlantic so we use data collected south of 12°N only. In addition, $fCO_2$ underway measurements were made during two zonal transects from Africa to French Guyana along 7°N and 7°30′N. Using these data, we assess the $CO_2$ variability in the western part of the NECC region, and in particular the occurrence of low $fCO_2$ and its origin. We also compute monthly seawater $fCO_2$ and air–sea $CO_2$ fluxes for the western tropical Atlantic using an empirical $fCO_2$—salinity relationship and climatological salinity fields. Zonal cruises and repeated France–Brazil voyages crossing the equator near 27°W provide more insights on the processes affecting the $CO_2$ undersaturation and its spatial and temporal variability.

## 2. Data and methods

During the CARBOOCEAN project, an automated $fCO_2$ instrument similar to the one described by Pierrot et al. (2009) has been installed in 2006 on the merchant ship *MN Colibri* sailing from Le Havre (France) to Kourou (located at 5°12′N, 52°46′W in French Guyana) and on the *Monte Olivia* sailing from Le Havre (France) to Santos (located at 23°58′S, 46°20′W in Brazil). The *MN Colibri* does not follow the same track on each voyage. In February–March, the track is further north, in April the ship sails further south and the track of the July and August voyages lies between the February and April tracks (Fig. 1). During the February voyage, the *MN Colibri* moved back and forth to Kourou before heading back to Le Havre so underway $fCO_2$ was measured at the same location several times. Eight voyages provided data in the western tropical Atlantic (Table 1). Along the France–Brazil line, the *Monte Olivia* follows always the same track and $fCO_2$ was measured underway from July 2008 to April 2009 during 11 voyages (Table 1). Both ships are equipped with a Seabird thermosalinograph recording sea surface temperature and salinity underway. Only $fCO_2$ data recorded between 10°S and 12°N have been used for this study.

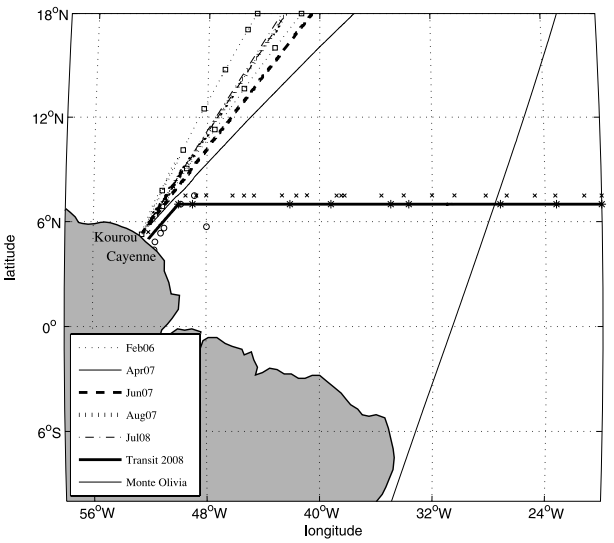


*Fig. 1.* Track of the voyages of the *MN Colibri* (in February–March 2006, April 2007, June 2007, August 2007, July 2008), of the zonal transit T08 along 7°N and of the *Monte Olivia* between 18°N and 10°S. The location of DIC and TA samples is indicated on the map. Samples were taken during the voyage of the Colibri in February–March 2006 (squares), the Plumand cruise (crosses), the transit in 2008 (stars) and the Amandes 1 cruise (open circles).

The $fCO_2$ was also measured underway during an eastward transect along 7°N from Cayenne to Cotonou (Benin) carried out from 1 to 17 August 2008 on board the *R/V Antea*. Underway oceanic and atmospheric $fCO_2$ were measured by infrared detection using a Licor 7000. The $fCO_2$ system uses an air–sea equilibrator described by Poisson et al. (1993). The measuring system was connected to the thermosalinograph. Seawater, pumped from 5 m deep, circulates in the equilibrator at a rate of 2 l min$^{-1}$. A closed loop of about 100 ml of air circulates as a countercurrent in the equilibrator designed in such a way that there is no bubbles at the air–sea interface (Poisson et al., 1993). To minimize temperature corrections, the equilibrator is thermostated with the same seawater as the one used for $CO_2$ measurements. The temperature difference between the equilibrator and the sea was less than 0.7 °C. The $fCO_2$ system was the same as the one used by Lefèvre (2009). The estimated accuracy of the seawater $fCO_2$ measurements was $\pm 2$ $\mu$atm. During the 2008 cruise, the mean atmospheric $fCO_2$ was $369.0 \pm 2.6$ $\mu$atm.

Samples for dissolved inorganic carbon (DIC) and alkalinity (TA) analyses were taken during the voyages of the Colibri in February–March 2006 as a scientist was on board. Seawater samples for DIC and TA analyses were also taken during a zonal transect and during a cruise on the Guyana shelf on board the *R/V Antea*. Surface seawater samples were taken from the Niskin bottles and the pumping line of the ship. There was no

*Table 1.* List of cruises made between 2006 and 2009 and used in this study

| Cruise | Dates | Measurements | Track | Vessel |
|---|---|---|---|---|
| Coli_Feb06 | 25 February–6 March 2006 | $fCO_2$, DIC, TA | Le Havre–Kourou | *MN Colibri* |
| | 8–26 March 2006 | $fCO_2$, DIC, TA | Kourou–Le Havre | |
| Coli_Apr07 | 20–30 April 2007 | $fCO_2$ | Le Havre–Kourou | *MN Colibri* |
| Coli_Jun07 | 11–19 June 2007 | $fCO_2$ | Le Havre–Kourou | *MN Colibri* |
| | 22–23 June 2007 | $fCO_2$ | Kourou–Le Havre | |
| Coli_Aug07 | 20–26 August 2007 | $fCO_2$ | Le Havre–Kourou | *MN Colibri* |
| Coli_Jul08 | 25 June–5 July 2008 | $fCO_2$ | Le Havre–Kourou | *MN Colibri* |
| | 19–26 July 2008 | $fCO_2$ | Kourou–Le Havre | |
| Monte_Jul08 | 25 June–5 July 2008 | $fCO_2$ | Le Havre–Santos | *Monte Olivia* |
| Monte_Aug08 | 4–12 August 2008 | $fCO_2$ | Santos–Le Havre | *Monte Olivia* |
| Monte_Oct08 | 3–13 October 2008 | $fCO_2$ | Le Havre–Santos | *Monte Olivia* |
| Monte_27Oct08 | 27 October–6 November 2008 | $fCO_2$ | Santos–Le Havre | *Monte Olivia* |
| Monte_Nov08 | 14–21 November 2008 | $fCO_2$ | Le Havre–Santos | *Monte Olivia* |
| Monte_Dec08 | 6–16 December 2008 | $fCO_2$ | Santos–Le Havre | *Monte Olivia* |
| Monte_27Dec08 | 27 December 2008–5 January 2009 | $fCO_2$ | Le Havre–Santos | *Monte Olivia* |
| Monte_Jan09 | 18–28 January 2009 | $fCO_2$ | Santos–Le Havre | *Monte Olivia* |
| Monte_Feb09 | 5–17 February 2009 | $fCO_2$ | Le Havre–Santos | *Monte Olivia* |
| Monte_Mar09 | 1–11 March 2009 | $fCO_2$ | Santos–Le Havre | *Monte Olivia* |
| Monte_Apr09 | 12–23 April 2009 | $fCO_2$ | Le Havre–Santos | *Monte Olivia* |
| Plumand | 10–20 October 2007 | DIC, TA | Abidjan–Cayenne | *R/V Antéa* |
| Amandes 1 | 25–26 October 2007 | DIC, TA | Cayenne–Cayenne | *R/V Antéa* |
| Transit NECC | 2–16 August 2008 | $fCO_2$ | Cayenne–Cotonou | *R/V Antéa* |

The *MN Colibri* and the *Monte Olivia* are merchant ships sailing from France to French–Guyana and France to Brazil, respectively. The Plumand and Transit NECC are zonal cruises along 7°30′N and 7°N, respectively, and the Amandes 1 cruise took place on the continental shelf of the Guyana coast.

difference in DIC and TA between the samples taken from the Niskin bottles and those from the pumping line, which suggests that there was no significant biofouling and respiration in the pumping lines. The westward transect along 7°30′N, between Abidjan (Ivory Coast) and Cayenne (French Guyana), took place from 10 to 21 October 2007. Due to a problem with the seawater $CO_2$ system, only atmospheric $fCO_2$ could be measured. The mean atmospheric $fCO_2$ was $366.9 \pm 2$ $\mu$atm. The cruise on the continental shelf of the Guyana coast, Amandes 1, was realized between 25 and 27 October 2008. With all these cruises, the seasonal cycle is almost complete (Table 1).

DIC and TA were measured by potentiometric titration using a closed cell, following the method of Edmond (1970). The equivalent points were calculated using the code published by DOE (1994). Certified Reference Material (CRM), supplied by Prof. A. Dickson (Scripps Institutions of Oceanography, San Diego, USA), were used for calibration. The accuracy was estimated at 3 $\mu$mol $kg^{-1}$.

During the France–French Guyana voyages on board the *MN Colibri*, atmospheric $fCO_2$ was contaminated by the fumes of the ship. For these cruises, we use the monthly molar fraction of $CO_2$, $xCO_{2atm}$, recorded at the atmospheric station at Ragged Point (13.17°N, 59.43°W) of the NOAA/ESRL Global Monitoring Division (http://www.esrl.noaa.gov/gmd/ccgg/iadv/), the monthly atmospheric pressure and the monthly SST of the NCEP/NCAR reanalysis project to calculate atmospheric $fCO_2$. For the zonal cruises and the France–Brazil cruises between 10°S and 10°N, the measured atmospheric $fCO_2$ was used. The atmospheric $xCO_2$ values recorded at Ragged Point and obtained with GLOBALVIEW-$CO_2$ (2009) are compared with the measured $xCO_2$ in the northern hemisphere (Fig. 2). There is relatively good agreement between the mean atmospheric $xCO_2$ measured during the cruises and recorded at Ragged Point, given the variability observed during the cruises. Overall, the $xCO_2$ measured during the cruises tend to be slightly higher than the values at the atmospheric station.

An acoustic Doppler current profiler (ADCP) measured the upper velocity continuously along the track during the transects in October 2007 and August 2008 on board the *R/V Antea*.

The Amazon discharge is monitored by the Environmental Research Observatory HYBAM (Geodynamical, hydrological and biogeochemical control of erosion/alteration and material transport in the Amazon basin, http://www.ore-hybam.org). The values recorded at the Obidos gauging station, located at about 600 km of the river mouth, are used to estimate the seasonal and the year-to-year variability of the Amazon outflow during the period of the cruises, from 2006 to 2008 (Fig. 3). The high-flow peaks in May–June and the low flow is observed between

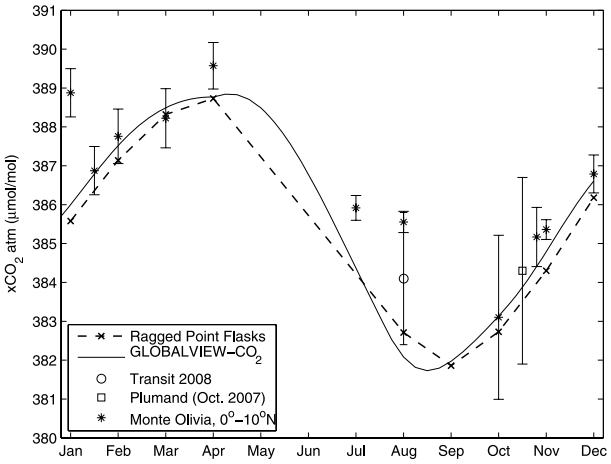


*Fig. 2.* Monthly atmospheric dry air molar fraction, $xCO_2$, from the atmospheric station Ragged Point, GLOBALVIEW-$CO_2$ and measured during the zonal cruises Plumand in October 2007 and Transit 2008, and during the France–Brazil cruises on board the *Monte Olivia* from 0°N to 10°N.

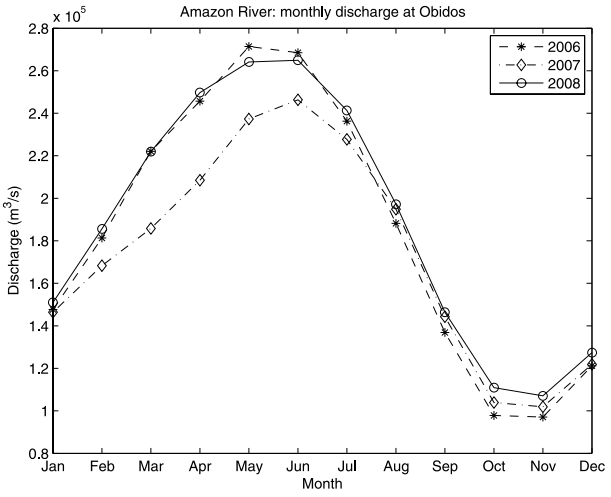


*Fig. 3.* Monthly discharge of the Amazon River recorded at the Obidos gauging station from 2006 to 2008 by the Environmental Research Observatory HYBAM (geodynamical, hydrological and biogeochemical control of erosion/alteration and material transport in the Amazon basin).

October and December. The monthly discharge is lower in 2007 compared to 2006 and 2008 from February to March. For the other months, there is no significant year-to-year variability from 2006 to 2008.

## 3. Distribution of the difference of $fCO_2$ between the ocean and the atmosphere

The longitudinal distributions of the difference of $fCO_2$ between the ocean and the atmosphere ($\Delta fCO_2$) of salinity and of temperature are shown for the two zonal cruises from 53°W to 30°W and for the France–French Guyana cruises south of 12°N which corresponds to the longitudinal range 47–53°W (Fig. 4). For comparison, the observations made during the Cither 1 cruise in February 1993 (Oudot et al., 1995) along 7°30′N and during the Meteor cruise 55 in October–November 2002 along 10°N (Körtzinger, 2003) are also presented.

Zonal cruises: the $\Delta fCO_2$ distribution of the zonal cruises exhibits a pronounced seasonal variability with a positive $\Delta fCO_2$ along 7°30′N, in February, for the whole transect of the Cither cruise, while $CO_2$ undersaturation is observed both in August and in October (Fig. 4a). In February, the salinity is much higher (Fig. 4b) with a mean value of 35.360 ± 0.382 and the SST much lower (26.28 ± 0.52 °C) compared to the other zonal cruises (Fig. 4c). In August, October and November, the SST can be higher than 29 °C while, in February, SST is always below 27 °C. The lowest salinities are measured close to the shelf near 50°W with values down to 25 in August 2008 and 30 in October 2002 due to the freshwater supply of the Amazon. A very low value around 30 is observed quite far east, near 40°W, in August 2008, and a $CO_2$ undersaturation is associated with this salinity decrease (Fig. 4b).

France–French Guyana cruises on the *MN Colibri*: the longitudinal distribution of $\Delta fCO_2$ for the France–French Guyana cruises shows a strong variability west of 50°W (Fig. 4d). The voyage made in August exhibits the strongest $CO_2$ undersaturation associated with a very low salinity (Figs d and e). However, August does not correspond to the highest Amazon discharge (Fig. 3), which suggests that the salinity distribution is also strongly related to the surface currents. The salinity in June is significantly lower than in February–March, which is consistent with the Amazon discharge, and decreases further in July and August. At this time of the year, the NBC starts its retroflection and Amazon waters spread offshore while, in February, the NBC is closer to the coast so that low salinities are observed only west of 52°W when the ship is close to the coast. The salinity in April is quite similar to the February–March values and starts decreasing slightly in June with lowest values west of 52°W. In July, the mean salinity is lower but remains above 29 while, in August, a strong decrease is observed near 51°30′W (SSS = 18) close to very high SSS (>35), further east, between 50°W and 51°W (Fig. 4e). The SST follows the seasonal cycle with the lowest values observed in February–March and increasing values towards the boreal summer. An interesting feature is the very high SST (>29 °C) associated with the lowest SSS in August 2007 between 52°W and 51°W and the decrease of SST (28 °C) between 51°W and 50°W (Fig. 4f) corresponding to a relatively high salinity (>35). Near 50°W, the increase in SST is associated with a decrease in salinity. Different water masses are sampled along this transect, the warm and fresh water is associated with Amazon waters while the salty and cooler water characterizes oceanic water. The wave pattern of the ocean circulation in this region, where eddies are often observed (Fratantoni and Glickson, 2001), explains the contrasting water masses encountered along

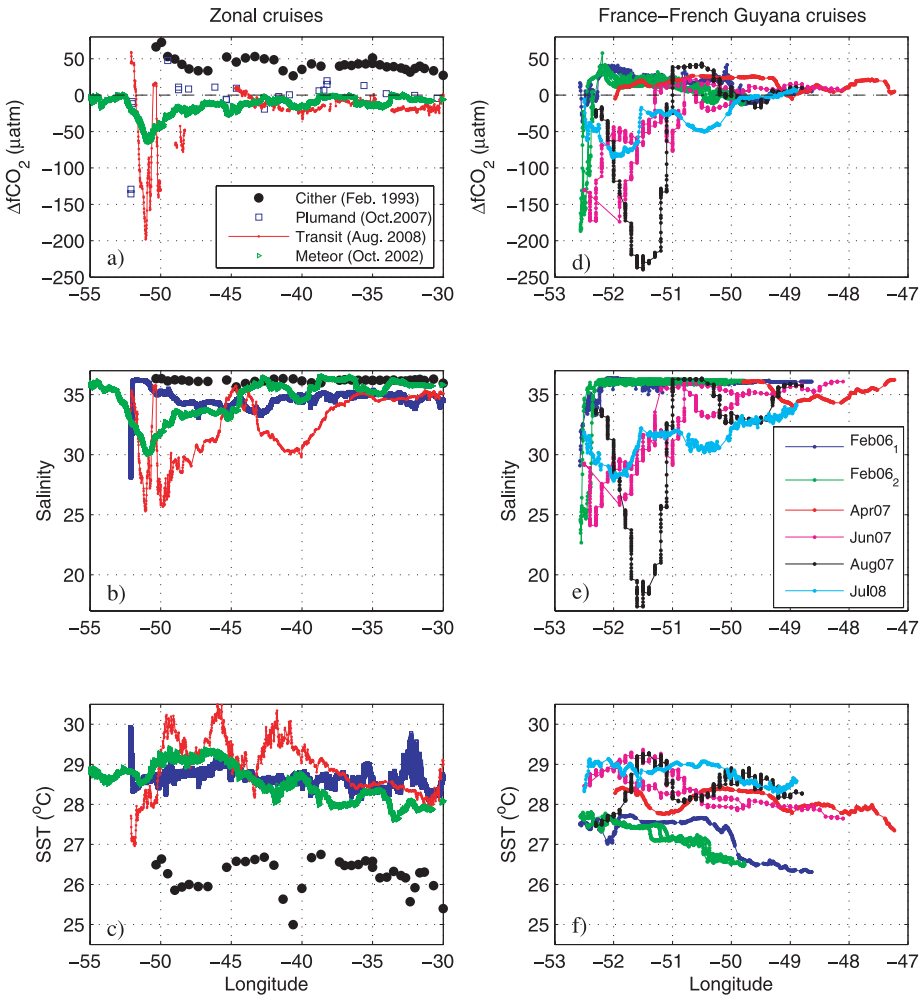


*Fig. 4.* Distribution of (a) $\Delta fCO_2$, (b) sea surface salinity and (c) sea surface temperature as a function of longitude for the zonal cruises. Distribution of (d) $\Delta fCO_2$, (e) sea surface salinity and (f) sea surface temperature as a function of longitude for the France–French Guyana voyages of the *MN Colibri*.

the ship track. During the France–French Guyana cruises, the $fCO_2$ distribution is very similar to the salinity variability suggesting that the $fCO_2$ variability could be driven by salinity changes in this area. In the next section, relationships between carbon parameters and salinity are investigated.

## 4. Salinity controls TA, DIC and $fCO_2$ variability west of 30°W and south of 12°N

Using the 38 alkalinity samples collected during the zonal transect along 7°30′N (Plumand), during the cruise on the continental shelf (Amandes 1) and during the France–French Guyana voyages west of 30°W and south of 12°N, we determine a relationship between alkalinity (TA) and sea surface salinity (SSS)

$$\mathrm{TA} = 58.1(\pm 0.5)\mathrm{SSS} + 265(\pm 18), \quad r^2 = 0.997, \qquad (1)$$

where the error on each coefficient is given in parentheses. The error on the predicted alkalinity is $\pm 11.6$ $\mu$mol kg$^{-1}$. Millero et al. (1998) determined a climatology of alkalinity for the world ocean. For the tropics, they give a normalized alkalinity NTA (=TA×35/SSS) constant to 2291 $\mu$M. Lee et al. (2006) determined a relationship between alkalinity and temperature and salinity for a salinity range 31–38. Our alkalinity relationship is in good agreement with both relationships for salinity higher than 31 but a strong discrepancy is observed at low salinity.

DIC and SSS are also highly correlated

$$\mathrm{DIC} = 50.6(\pm 0.9)\mathrm{SSS} + 189(\pm 31), \quad r^2 = 0.988 \qquad (2)$$

with an error of $\pm 16.2$ $\mu$mol kg$^{-1}$ on the prediction of DIC. The data point at SSS = 20 obtained on the continental shelf (during Amandes 1) was not taken into account in calculating

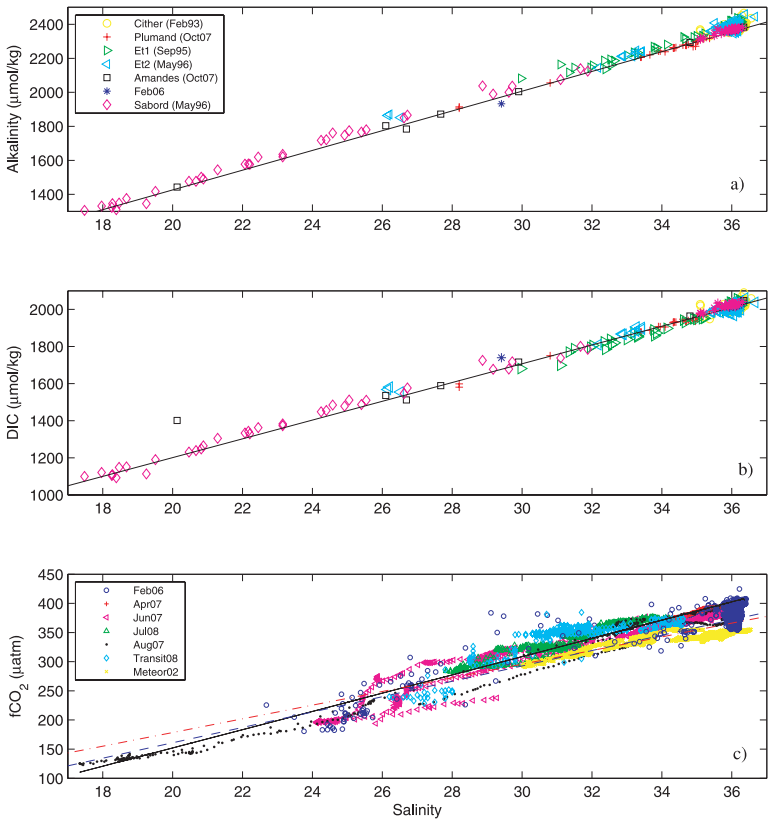


*Fig. 5.* (a) Alkalinity as a function of salinity, (b) DIC as a function of salinity for the Cither, Sabord, Etambot 1, Etambot 2, Colibri February–March 2006, Plumand and Amandes 1 cruises. The solid line corresponds to the fit using only the Colibri February–March 2006, Plumand and Amandes data. (c) $fCO_2$ as a function of salinity for the Colibri voyages in February leg 1, February leg 2 (squares), April 2007, June 2007, July 2008, August 2007 and the zonal cruises along 7°N in August 2008 (transit 2008) and along 10°N in November 2002 (Meteor02). The solid line is the fit using all the data except the Meteor cruise.

the DIC–SSS regression as it seems to be an outlier for DIC (Fig. 5).

DIC and TA have been measured during the Cither 1 cruise along 7°30′N (Oudot et al., 1995), as well as during the Etambot 1 and 2 and Sabord cruises made in February 1993, September–October 1995, April–May 1996 and May 1996 respectively, in the tropical Atlantic (Ternon et al., 2000). The Etambot 1 and 2 cruises sampled the region between 8°S and 8°N, west of 35°W and the Sabord cruise took place on the continental shelf off French Guyana. The DIC and TA observations of these cruises are reported on the TA–SSS, DIC–SSS plots (Figs 5a and b). Both relationships are quite robust as shown by the good agreement between the regression and the available observations from previous cruises. The TA–SSS and DIC–SSS regressions were performed for salinities greater than 20 and 26, respectively, but the Sabord data obtained in May 1996 have salinity ranging from 18 to 27 and are very close to the fit line (Figs 5a and b). Ternon et al. (2000) reported TA–SSS and DIC–SSS slopes of, respectively, 58.85 and 49.48 $\mu$mol kg$^{-1}$ using the data from Etambot 1 and 2 and Sabord cruises.

As the distribution of $fCO_2$ exhibits similar patterns to the salinity variations, all the underway $fCO_2$ measurements ($N = 5288$) from the France–French Guyana cruises and the 2008 zonal transect were used to determine a $fCO_2$–SSS relationship in the salinity range from 17 to 36.5 and for $fCO_2$ values between 120 and 425 $\mu$atm encountered during the cruises. The temperature ranges from 26 to 30 °C with a mean of 27.94 ± 0.80 °C. As the variability of temperature is small compared to the variability of salinity, $fCO_2$ can be expressed as a function of salinity only.

The following regression is obtained:

$$fCO^2 = 13.4(\pm 0.1)SSS - 97(\pm 2), \quad r^2 = 0.90 \tag{3}$$

with an error of ±15.5 $\mu$atm in estimating $fCO_2$. This is very close to the relationship obtained by Körtzinger (2003) but if we use only salinity less than 35, as he did, the number of observations is reduced to 2314 and the equation becomes

$$fCO^2 = 15.7(\pm 0.1)S - 161(\pm 3), \quad r^2 = 0.92 \tag{4}$$

with an error of ±14.0 $\mu$atm in predicting $fCO_2$. There is less dispersion when using SSS less than 35, even if the dispersion remains quite high (Fig. 5c), and the fit is slightly improved. However, the slope of the regression line becomes higher with a value of 15.7 $\mu$atm psu$^{-1}$ compared to 13.18 $\mu$atm psu$^{-1}$ obtained by Körtzinger (2003), and 11.72 $\mu$atm psu$^{-1}$ by Ternon et al. (2000). The salinity dependence of $fCO_2$ in the western tropical Atlantic, under Amazon influence, is very different from the equatorial region with no river influence. Oudot et al. (1987)

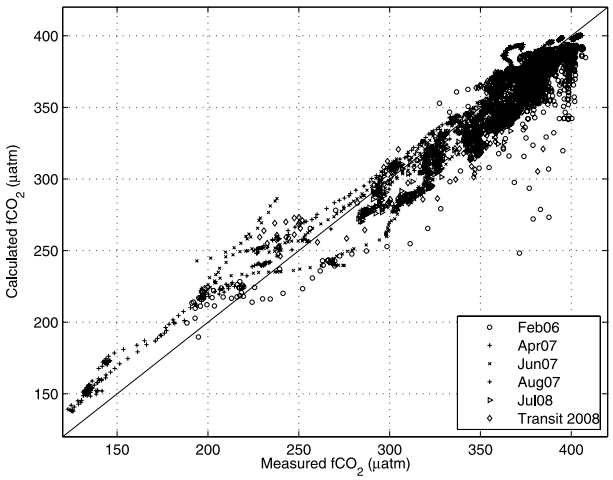


*Fig. 6.* $fCO_2$ calculated from DIC and TA, using eqs. (1) and (2) and observed temperature and salinity data, as a function of observed $fCO_2$ from the cruises used in Fig. 5c. The solid line is the 1:1 line.

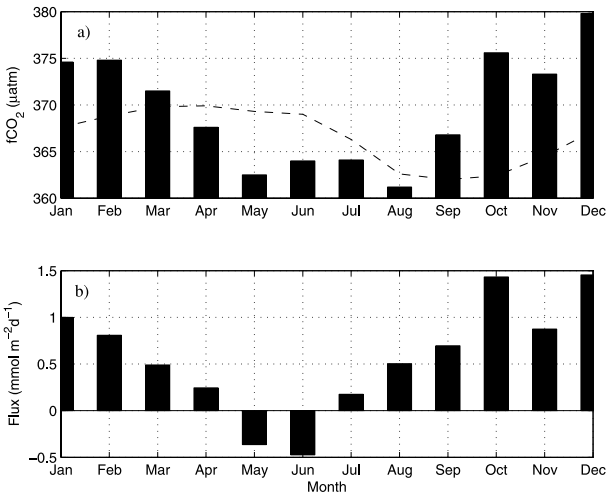


*Fig. 7.* (a) Monthly means of seawater $fCO_2$ calculated with the $fCO_2$–SSS relationship, the dashed line corresponds to the atmospheric value calculated from the Ragged Point atmospheric station. (b) Monthly $CO_2$ flux for the region 65°W–35°W, 5°S–10°N. The solid line corresponds to no exchange and a negative $CO_2$ flux to a sink of $CO_2$ for the atmosphere.

reported a dependence of 44 $\mu$atm psu$^{-1}$ for the equatorial Atlantic (5°S–5°N) comparable to the 40 $\mu$atm psu$^{-1}$ obtained by Fushimi (1987) in the western Pacific.

The measured $fCO_2$ is compared with $fCO_2$ calculated from DIC and TA using eqs. (1) and (2) and the observed SST and S data (Fig. 6). The calculated values tend to be higher than the observed ones for low $fCO_2$ (<200 $\mu$atm) whereas calculated values tend to underestimate the observed ones for high $fCO_2$ associated with high salinity.

## 5. $CO_2$ flux in the western tropical Atlantic

Using the monthly fields of sea surface salinity from the World Ocean Atlas 2005 (Antonov et al., 2006), $fCO_2$ can be calculated using eq. (3). This equation is applied only to salinity higher than 15 and for the region between 65–35°W and 5°S–10°N. This domain was considered previously by Ternon et al. (2000) for extrapolation because it corresponds to the low-salinity area as observed from the SSS climatology (Dessier and Donguy, 1994) and because the influence of the Amazon discharge can reach 35°W.

The $CO_2$ flux (in mol m$^{-2}$ yr$^{-1}$) is calculated as

$$\mathrm{fCO}^2 = kS(\mathrm{fCO}_{2_{\mathrm{sw}}} - \mathrm{fCO}_{2_{\mathrm{atm}}}), \tag{5}$$

where $k$ is the gas transfer velocity, $S$ is the gas solubility given by Weiss (1974), $fCO_{2sw}$ is the seawater $fCO_2$ calculated with the monthly salinity fields and $fCO_{2atm}$ is the atmospheric value calculated from the monthly molar fraction recorded at the Ragged Point station in 2007 as described in Section 2. Monthly maps of the gas exchange coefficient, $kS$, are provided by Boutin et al. (2009) using the QuikSCAT wind speed. The map used is calculated with the gas transfer velocity of Wanninkhof (1992). Following a new analysis of $^{14}$C measurements, Sweeney et al. (2007) proposed a new relationship for the gas transfer velocity

$$k = 0.27U^2(660/\mathrm{Sc})^{0.5}, \tag{6}$$

where $U$ is the wind speed at 10 m and Sc is the $CO_2$ Schmidt number. This gas transfer velocity corresponds to 0.87 times the gas transfer velocity of Wanninkhof (1992). The map provided by Boutin et al. (2009) was then multiplied by 0.87 to use the relationship of Sweeney et al. (2007).

On monthly average, the lowest salinities occur between May and August, which corresponds to the Amazon high flow whereas low flow takes place between September and December (Seyler et al., 2003). In 2007, the highest flow is in June and the lowest in November (Fig. 3). Therefore, the lowest seawater $fCO_2$ computed from salinity are between May and August (Fig. 7a). However, the winds are also the lowest during that period so that the $CO_2$ flux remains quite small with a sink of $CO_2$ in May and June, on monthly average (Fig. 7b). Monthly means $fCO_2$ in April, July and August are below the atmospheric level but when calculating the monthly average of the $CO_2$ flux, a small source is obtained because of the distribution of the wind speed. Salinity can be as low as 15 so $\Delta fCO_2$ can reach $-250$ $\mu$atm leading, on monthly average, to a negative $\Delta fCO_2$. However, the wind associated with these few very extreme values are low so that, on monthly average, the $CO_2$ flux is positive. The distribution of the $CO_2$ flux is different from the one of Ternon et al. (2000) as they calculated a strong negative $CO_2$ flux in April associated with a monthly mean salinity around 34. On annual average, they computed a sink of $CO_2$ of $0.12 \pm 0.57$ mmol m$^{-2}$ d$^{-1}$ using climatological wind speed and the gas exchange coefficient of Wanninkhof (1992), whereas we obtain a source

of $CO_2$ of 0.57 mmol $m^{-2}$ $d^{-1}$ with a standard deviation of 0.61 mmol $m^{-2}$ $d^{-1}$. The variability of the $CO_2$ flux is so high that on annual average both estimates agree within one standard deviation. For salinities over 24, our $fCO_2$–S relationship gives higher $fCO_2$ than the relationship used by Ternon et al. (2000). In addition, their atmospheric value of 353 $\mu$atm in 1996 is quite high. This corresponds to an atmospheric increase of 1.3 $\mu$atm $yr^{-1}$ between 1996 and 2007 and only 0.7 $\mu$atm $yr^{-1}$ between 1996 and 2002 as Körtzinger (2003) used an atmospheric value of 357.1 $\mu$atm for 2002. On monthly average, over a large region of the western tropical Atlantic (65–35°W, 5°S–10°N), the impact of the Amazon is mainly visible in spring as it is the high flow period. The mean seawater $fCO_2$ is lower than the atmospheric level during that period, however, as the winds are also quite weak, the $CO_2$ sink remains small.

Following the method of Körtzinger (2003) and defining the Amazon river plume by salinities less than 34.9, $fCO_2$ is calculated from salinity using eq. (4) in the region 3°S–18°N, 60–30°W, which is the domain considered by Körtzinger (2003). The Amazon plume is a strong sink of $CO_2$ with an annual flux of $-0.96 \pm 1.20$ mmol $m^{-2}$ $d^{-1}$. This estimate is lower than the $-1.35$ mmol $m^{-2}$ $d^{-1}$ obtained by Körtzinger (2003). The $CO_2$ flux integrated over the region where salinity ranges between 15 and 34.9 becomes $-0.005$ Pg C $yr^{-1}$ which is less than the $-0.014$ GC $yr^{-1}$ given by Körtzinger (2003). Using the annual salinity field of World Ocean Atlas 2005, only 89 grid cells have salinities ranging between 15 and 34.9, within the region 3°S–18°N, 60–30°W, which corresponds to a much smaller area, 1.1 $10^6$ $km^2$, than the $2.4 \times 10^6$ $km^2$ used in the calculation by Körtzinger (2003).

## 6. Eastward propagation of Amazon waters

The Amazon plume is transported according to the ocean circulation. In boreal winter, the plume remains close to the shelf whereas in summer it starts spreading northeastward. As $CO_2$ gas exchange is slow, the Amazon signature can be observed far from the mouth. In this section, we determine the amount of river water mixing with oceanic waters and its offshore propagation. The river endmember ($S = 0$) and the ocean endmember need to be determined to assess the mixing between the two water masses. The ocean endmember is determined when seawater and atmospheric $fCO_2$ are close, as done by Ternon et al. (2000) and Körtzinger (2003). This corresponds to a salinity of 34.7.

The mixing between ocean and river waters can be expressed with the following system of equations:

$$r S_r + s S_s = S_{\text{obs}}, \tag{7}$$

$$r + s = 1, \tag{8}$$

where $r$ is the fraction of riverine water and $s$ the fraction of seawater, $S_{\text{obs}}$ is the observed salinity. The freshwater changes by precipitation and evaporation are neglected compared to the freshwater supply of the river. Solving the two equations gives the percentage of Amazon water that is observed at the sampling locations.

Assuming a conservative mixing of surface alkalinity, an alkalinity river endmember of $265 \pm 18$ $\mu$mol $kg^{-1}$ can be determined at $S = 0$ from eq. (1). Surface TA is related to surface salinity in the world ocean but the TA–S relationship varies according to the ionic composition. A departure from the TA–S relationship is observed when calcifying organisms are present because of the precipitation of calcium carbonate. In the western tropical Atlantic, the primary production is essentially carried by diatoms (Cooley et al., 2007), so the conservative mixing of alkalinity is a reasonable assumption. There are very few alkalinity measurements available for the Amazon River. Most of the measurements are far upstream the Amazon and show a large variability (e.g. Devol et al., 1995). Cooley et al. (2007) reported a mean alkalinity of $360 \pm 55$ $\mu$mol $kg^{-1}$ at Macapá, close to the river mouth, using a dilution model. This is higher than our estimate of river alkalinity.

The percentage of river supply is highly variable. The Amazon water is more present in July and August during the France–French Guyana voyages of the *MN Colibri*. At this time of the year, the retroflection of the NBC starts so Amazon waters appear further offshore than in February. The zonal cruises took place in August and October during the period of the NBC retroflection. The surface velocity measured along the tracks shows the pattern of the NECC with a weaker eastward flow in October (Fig. 8a) compared to August (Fig. 8b). In addition, the Amazon discharge is stronger in August than in October (Fig. 3). In October 2007, the percentage of river water drops quickly with almost no Amazon waters east of 49°W (Fig. 8c) while in August 2008, Amazon waters can be observed near 40°W (Fig. 8d). At this location, the corresponding salinity is 30. The percentage of river outflow as a function of longitude shows that there was a greater extent of Amazon outflow during August 2008 compared to October 2007. Although both cruises took place during the retroflection of the NBC, the eastward propagation of Amazon waters is closely linked to the strength and direction of the NECC as shown by the ADCP measurements. A striking feature of the surface current is the lack of well-developed zonal component. The current field exhibits a wave structure with alternate northward and southward components of the eastward flow. This is consistent with previous observations of the propagation of surface waters as NBC rings (Fratantoni and Glickson, 2001). In August 2008, the current is close to zero at 45°W and no Amazon water is observed while at 40°W, when Amazon water is observed, the current is stronger with a northeastward direction.

In August 2008, $CO_2$ undersaturation was observed on a large longitudinal range whereas in October 2007, the dominant pattern was a source of $CO_2$. This is consistent with a stronger river advection in August 2008 compared to October 2007. During the zonal cruise, Cither, in February 1993 along 7°30′N, a source of

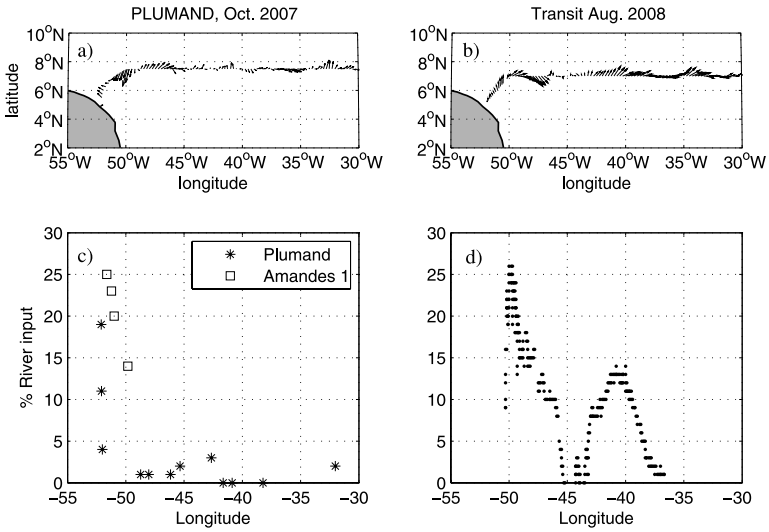


*Fig. 8.* (a) Surface currents measured during (a) October 2007, (b) August 2008 and percentage of river input as a function of longitude in (c) October 2007 and (d) August 2008.

$CO_2$ was observed (Oudot et al., 1995) and the salinity remains higher than 35 (Fig. 4b). This can be explained by the absence of the NECC west of 18°W at this time of the year (Richardson and Reverdin, 1987) and the position of the ITCZ south of the equator. In November, $CO_2$ undersaturation is observed along 10°N during the Meteor cruise probably as a result of the Amazon outflow (Körtzinger, 2003) and the ITCZ position close to 10°N.

## 7. Extent of undersaturation area

The Amazon plume creates $CO_2$ undersaturation that can be observed close to the shelf when the NBC transports the water mass to the Caribbean and remains close to the coast. Offshore transport is observed from July when the NBC starts its retroflection. During the France–French Guyana cruises, in February–March north of 5°30′N there is no more Amazon waters, salinity is close to 35. In July and August, a significant amount of fresh waters is observed along the track. At this time of the year, the start of the retroflection of the North Brazil Current entrains Amazon waters eastward. Up to 50% of river water is observed in August 2007 near 7°N.

Although no Amazon water was sampled east of 36°W in 2007 and 2008 (Figs 8c and d), $CO_2$ undersaturation is observed further east along the track of the France–Brazil line in the NECC region between 25°W and 30°W. The latitudinal distribution of $\Delta fCO_2$ from 10°S to 10°N shows $CO_2$ undersaturation north of about 2°N (Figs 9a–c) whereas, south of 2°N, $\Delta fCO_2$ is mostly positive except in July–August near 8–10°S (Fig. 9a). For the region between 10°S and 2°S, the $\Delta fCO_2$ distribution follows the seasonal cycle. In July and August, the austral winter, the temperatures are the lowest, around 27 °C (Fig. 9d). Then, they gradually increase (Fig. 9e) to become maximum between January and April with monthly means over 28 °C (Fig. 9f). This seasonal temperature increase is associated with a seawater $fCO_2$ increase. In July–August, $\Delta fCO_2$ is even negative between 7°S and 10°S (Fig. 9a) when the temperature is around 26 °C (Fig. 9d), then $\Delta fCO_2$ increases towards October–November (Fig. 9b) and the highest $fCO_2$ occur in austral summer from January to April (Fig. 9c). In the northern part of the section, between 2°N and 10°N, SST decreases at the end of December (Fig. 9e) to reach values around 24 °C in January–April (Fig. 9f). $\Delta fCO_2$ is always negative between 5°N and 8°N (Figs 9a–c). In July–August, the undersaturation is located between 2°N and 8°N, then it moves northwards between 3°N and 10°N in January–April. Low salinities are encountered with salinities less than 35 from July to December between 2°N and 8°N (Figs 9g and h) whereas, from January to April, salinities less than 35 are observed south of the equator (Fig. 9i). From January to April the negative $\Delta fCO_2$ between 5°N and 10°N are explained by the winter cooling and not by salinity. Salinity is above 35 because, during this period, the ITCZ is near 2°S. This is consistent with the observed decrease of salinity (Fig. 9i) and with the analysis of precipitation data in the tropical Atlantic by Gu and Adler (2006). Normalizing $fCO_2$ to a constant temperature leads to near-equilibrium conditions. Overall, between 10°S and 2°S the monthly mean salinity ranges from 35.48 to 36.18 and is always higher than in the 2–10°N latitudinal band. The low-salinity region is associated with a decrease of $\Delta fCO_2$. The eastward propagation of Amazon waters is unlikely to explain the $CO_2$ undersaturation observed throughout the year because Amazon waters might reach 25–30°W in boreal autumn, depending on the strength of the NECC, but at other seasons, the NBC entrains Amazon waters towards the Caribbean. As the NECC disappears or reverses near 18°W from January to June (Richardson and Reverdin, 1987), Amazon waters cannot be transported eastward.

In the tropical region, Oudot et al. (1987) explained $CO_2$ undersaturation associated with low salinities by the presence of the intertropical convergence zone (ITCZ). The ITCZ attains

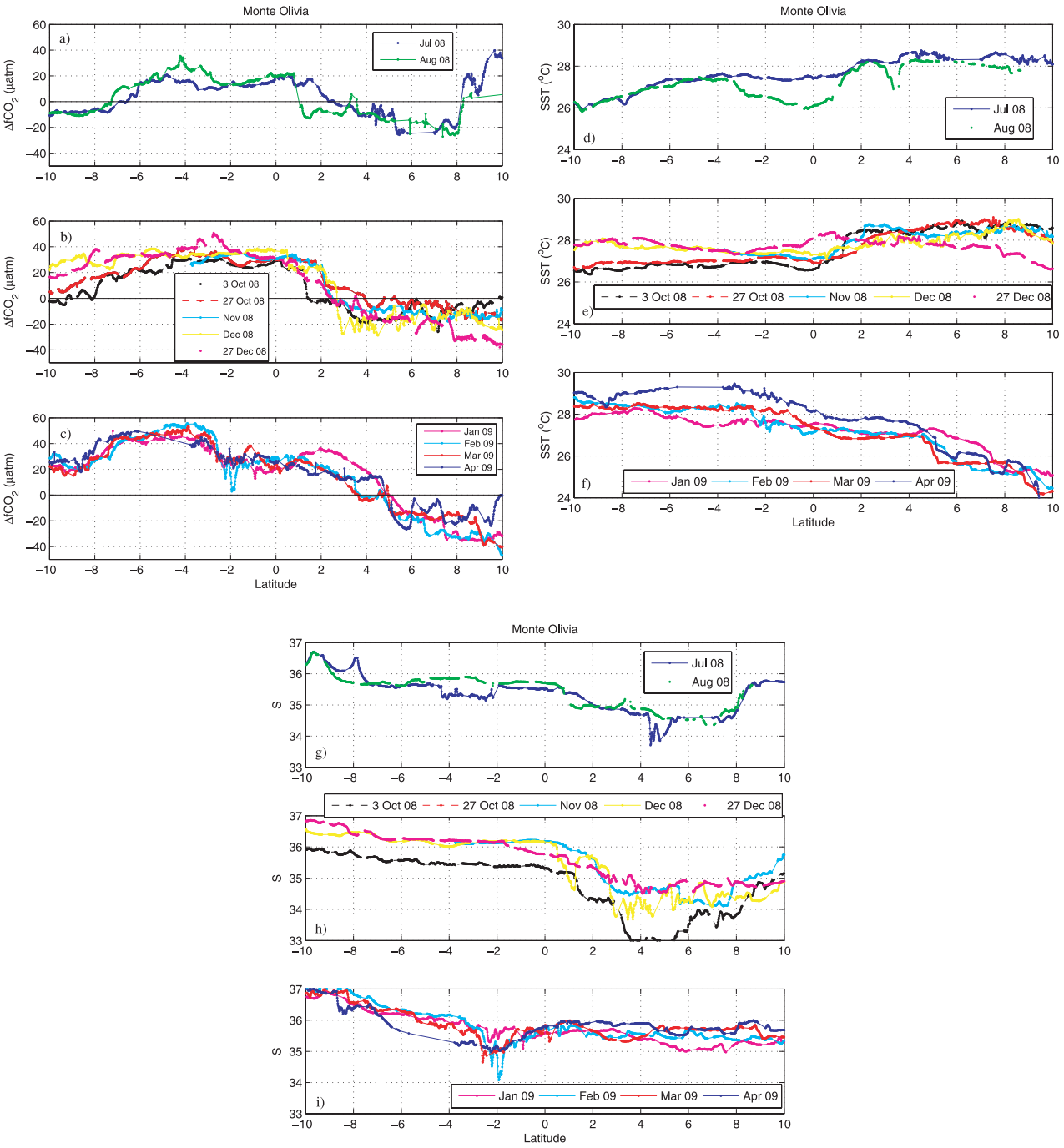


*Fig. 9.* Distribution of $\Delta fCO_2$ between 10°S and 10°N along the track of the France–Brazil line for (a) July and August 2008, (b) October to December 2008 and (c) January to April 2009. Distribution of SST for (d) July and August 2008, (e) October to December 2008 and (f) January to April 2009. Distribution of salinity for (g) July and August 2008, (h) October to December 2008 and (i) January to April 2009.

its southernmost position during March–April and it migrates northward in July–August (Gu and Adler, 2006). The ITCZ is associated with high precipitation, which explains the lower surface salinity observed in March compared to the August and October cruises (Fig. 10a). The migration of the ITCZ is consistent with the salinity distribution with low salinities located north of 2°N from July to December (Figs 9g and h) and near 2°S from January to April (Fig. 9i).

During August and October, the ITCZ is at its northernmost location. The monthly climatology of precipitation (Adler et al.,

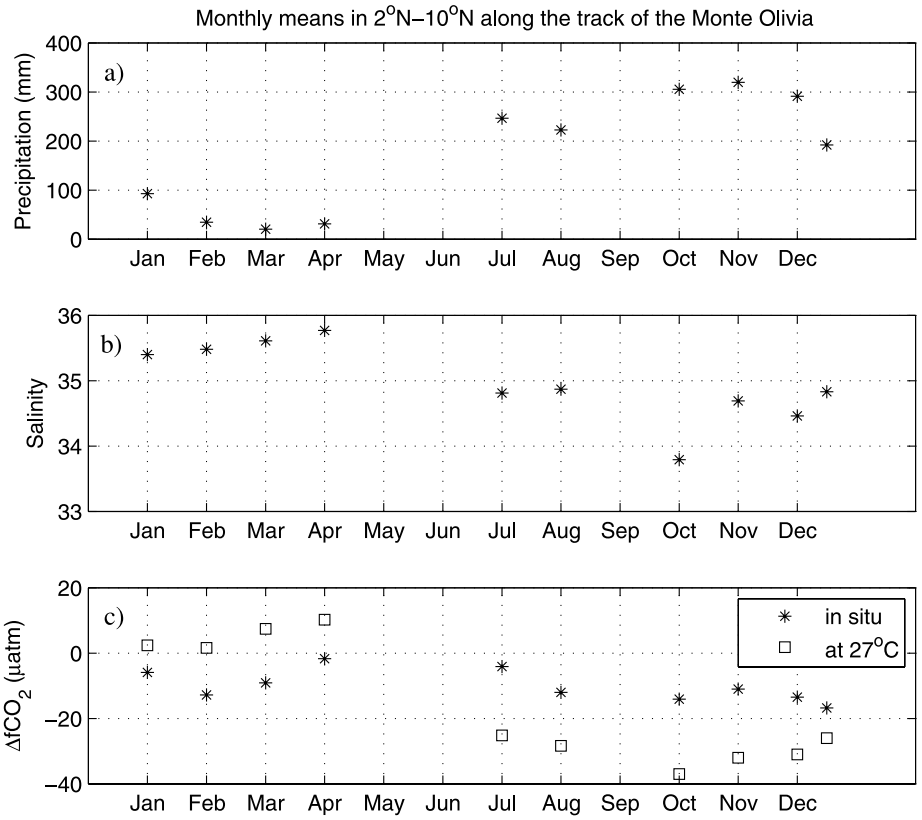


*Fig. 10.* Monthly means of (a) precipitation, (b) sea surface salinity and (c) $\Delta fCO_2$ at seawater temperature and at a constant temperature of 27 °C, between 2°N and 10°N along the track of the France–Brazil line. The precipitation data come from the Global Precipitation Climatology Project (GPCP) version 2.1 data set (Adler et al., 2003).

2003) averaged in the NECC region between 2°N and 10°N shows low values in January–March and high values in boreal autumn which is consistent with the seasonal migration of the ITCZ. The monthly mean sea surface salinity measured on the France–Brazil line is correlated with precipitation ($r^2 = 0.82$). The higher salinities are observed during the months of low precipitation whereas low salinities are observed in boreal autumn when high precipitation occurs (Fig. 10b). The monthly mean $\Delta fCO_2$ are not strongly correlated with salinity ($r^2 = 0.31$), although we expect low seawater $fCO_2$, hence low $\Delta fCO_2$, to be associated with low salinity. This is explained by the temperature effect. In winter, low precipitation leads to high salinity, which should lead to high $fCO_2$. However, the low temperatures would tend to decrease $fCO_2$ and counterbalance the salinity effect. After removing the temperature effect using the 4% per °C relationship (Takahashi et al., 1993), the $\Delta fCO_2$ calculated at a temperature of 27 °C is strongly correlated with salinity ($r^2 = 0.85$) with a sink of $CO_2$ from July to December when the salinity is lower than 35 and a source of $CO_2$ from January to April when the salinity is over 35. This confirms that the $CO_2$ undersaturation observed in the NECC region along the track of the France–Brazil line is caused by the precipitation due to the presence of the ITCZ.

In boreal autumn, both the Amazon discharge and the position of the ITCZ can lead to $CO_2$ undersaturation. In boreal winter, January–March, $CO_2$ undersaturation might occur in the NECC region due to winter cooling. The next step would be to synthesize all the available cruises made in this region to assess the impact of the $CO_2$ undersaturation on the tropical source of $CO_2$. The surface ocean $CO_2$ atlas project (SOCAT) has started building an $fCO_2$ database that could address this issue. Pursuing the monitoring of the region with the France–Brazil line will determine whether the $CO_2$ undersaturation reported here between 5°N and 8°N throughout the year is a permanent feature. There might be some year-to-year variability as no $CO_2$ undersaturation was observed during the zonal cruise along 7°30′N in February 1993.

## 8. Conclusions

Underway $fCO_2$ measurements collected on board two merchant ships and during research cruises show area of $CO_2$ undersaturation in the region of the NECC. In the western tropical Atlantic, the strong salinity dependence of TA, DIC and $fCO_2$, and the large salinity range are explained by the freshwater supply of the Amazon. The lowest $fCO_2$ is correlated with the lowest salinity

confirming that most of the productivity comes from the river. Relationships between TA, DIC and $fCO_2$ could be determined and seem to be valid throughout the year. Using mean sea surface salinity fields, an annual sink of $-0.96$ mmol $m^{-2}$ $d^{-1}$ could be calculated for the Amazon plume, defined by salinities below 34.9, in the region 3°S–18°N, 60–30°W.

The eastward propagation of Amazon waters could be examined during two cruises made along 7°30′N in October 2007 and 7°N in August 2008 during the period of the NBC retroflection. The percentage of Amazon water advected eastwards depends on the strength of the NECC and follows a wave pattern. In August 2008, a stronger NECC and a stronger Amazon discharge than in October 2007 explain the presence of Amazon waters at 40°W associated with a salinity of 30.

Further east, along the track of the France–Brazil line, $CO_2$ undersaturation is observed throughout the year in the NECC region between 25°W and 30°W. It is associated with low salinities and can be explained by the high precipitation due to the presence of the ITCZ. After removing the temperature effect, a clear seasonal pattern emerges with low precipitation, salinities over 35 and high $fCO_2$ observed in boreal winter when the ITCZ is located further south, and high precipitation, salinities below 35 and low $fCO_2$ from July to December under the ITCZ.

Continuing the monitoring with the merchants ships and with the mooring at 8°N, 38°W should better document the variability of these area of low $fCO_2$ in the NECC, their location and their extent. Synthesizing all the data available in this region will help in assessing the impact of the $CO_2$ undersaturation on the source of $CO_2$ in the tropical Atlantic. This should be addressed in the Surface Ocean $CO_2$ Atlas Project.

## 9. Acknowledgments

We thank the Compagnie Maritime Nantaise (MN) and the Hamburg Süd shipping companies for allowing the installation of our $CO_2$ equipment on board their ships. We are very grateful to the officers and crew of the *MN Colibri*, the *Monte Olivia* and the *R/V Antea* for their help on board with the measurements. Precipitation data from the Global Precipitation Climatology Project (GPCP) were downloaded from the Giovanni online data system, developed and maintained by the NASA Goddard Earth Sciences (GES) Data and Information Services Center (DISC). We also acknowledge the TRMM mission scientists and associated NASA personnel for production of the data used in this research effort. NCEP reanalysis derived data and NOAA_OI_SST_V2 data were provided by the NOAA/OAR/ESRL PSD, Boulder, Colorado, USA, from their Web site at http://www.esrl.noaa.gov/psd/. DIC and TA analyses were realized by the SNAPO-$CO_2$ at LOCEAN. We acknowledge support from the European Integrated Project CARBOOCEAN (contract 511176–2), the Institut de Recherche pour le Développement (IRD) and the national program LEFE CYBER. The paper benefited from the comments of three anonymous reviewers.

## References

Adler, R. F., Huffman, G. J., Chang, A., Ferraro, R., Xie, P. and co-authors. 2003. The version 2 Global Precipitation Climatology Project (GPCP) Monthly Precipitation Analysis (1979-Present). *J. Hydrometeor.* **4**, 1147–1167.

Andrié, C., Oudot, C., Genthon, C. and Merlivat, L. 1986. $CO_2$ fluxes in the tropical Atlantic during FOCAL cruises. *J. Geophys. Res.* **91**(C10), 11741–11755.

Antonov, J. I., Locarnini, R. A., Boyer, T. P., Mishonov, A. V. and Garcia, H. E. 2006. World Ocean Atlas 2005. In *NOAA Atlas NESDIS 62* U.S. Government Printing Office, Washington, DC, 182.

Boutin, J., Quilfen, Y., Merlivat, L. and Piolle, J. F. 2009. Global average of air-sea $CO_2$ transfer velocity from QuikSCAT scatterometer wind speeds. *J. Geophys. Res.* **114**(C4007), doi:10.1029/2007JC004168.

Cooley, S. R., Coles, V. J., Subramaniam, A. and Yager, P. L. 2007. Seasonal variations in the Amazon plume-related atmospheric carbon sink. *Global Biogeochem. Cycles* **21**, doi:10.1029/2006GB002831.

Demaster, D. J., Smith, W. O. Jr, Nelson, D. M. and Aller, J. Y. 1996. Biogeochemical processes in Amazon shelf waters: chemical distributions and uptake rates of silicon, carbon and nitrogen. *Cont. Shelf Res.* **16**(5/6), 617–643.

Dessier, A. and Donguy, J. R. 1994. The sea surface salinity in the tropical Atlantic between 10°S and 30°N—seasonal and interannual variations (1977–1989). *Deep-Sea Res.* **41**(1), 81–100.

Devol, A. H., Forsberg, B. R., Richey, J. and Pimentel, T. P. 1995. Seasonal variation in chemical distributions in the Amazon (Solimões) River: a multiyear time series. *Global Biogeochem. Cycles* **9**(3), 307–328.

DOE, *Handbook of Methods for the Analysis of the Various Parameters of the Carbon Dioxide System in Sea Water* ORNL/CDIAC-74, 1994.

Edmond, J. M. 1970. High precision determination of titration alkalinity and total carbon dioxide content of seawater by potentiometric titration. *Deep-Sea Res.* **17**, 737–750.

Fratantoni, D. M. and Glickson, D. A. 2001. North Brazil Current ring generation and evolution observed with SeaWiFS. *J. Phys. Oceanogr.* **32**, 1058–1074.

Fushimi, K. 1987. Variation of carbon dioxide partial pressure in the western North Pacific surface water during the 1982/83 El Niño event. *Tellus* **39B**, 214–227.

GLOBALVIEW-$CO_2$ 2009. Cooperative Atmospheric Data Integration Project – Carbon Dioxide. *CD-ROM, NOAA ESRL, Boulder, Colorado* Also available on internet via anonymous ftp to ftp.cmdl.noaa.gov, path:ccg/co2/GLOBALVIEW.

Gu, G. and Adler, R. F. 2006. Interannual rainfall variability in the tropical Atlantic region. *J. Geophys. Res.* **111**(D02106), doi:10.1029/2005JD005944.

Körtzinger, A. 2003. A significant sink of $CO_2$ in the tropical Atlantic Ocean associated with the Amazon River plume. *Geophys. Res. Lett.* **30**(24), 2287, doi:10.1029/2003GL018841.

Lee, K., Tong, L. T., Millero, F. J., Sabine, C., Dickson, A. G. and co-authors. 2006. Global relationships of total alkalinity with salinity and temperature in surface waters of the world's oceans. *Geophys. Res. Lett.* **33**(L19605), doi:10.1029/2006GL027207.

Lefèvre, N. 2009. Low $CO_2$ concentrations in the Gulf of Guinea during the upwelling season in 2006. *Mar. Chem.* **113**, 93–101.

Lefèvre, N., Moore, G., Aiken, J., Watson, A., Cooper, D. and co-authors. 1998. Variability of $pCO_2$ in the tropical Atlantic in 1995. *J. Geophys. Res.* **103**(C3), 5623–5634.

Mayorga, E., Aufdenkampe, A. K., Masiello, C. A., Krusche, A. V., Hedges, J. I. and co-authors. 2005. Young organic matter as a source of carbon dioxide outgassing from Amazonian rivers. *Nature* **436**, 538–541.

Millero, F. J., Lee, K. and Roche, M. 1998. Distribution of alkalinity in the surface waters of the major oceans. *Mar. Chem.* **60**, 111–130.

Oudot, C., Andrié, C. and Montel, Y. 1987. Evolution du $CO_2$ océanique et atmosphérique sur la période 1982–1984 dans l'Atlantique tropical. *Deep-Sea Res.* **34**(7), 1107–1137.

Oudot, C., Ternon, J. F. and Lecomte, J.. 1995. Measurements of atmospheric and oceanic $CO_2$ in the tropical Atlantic: 10 years after the 1982–1984 FOCAL cruises. *Tellus* **47B**, 70–85.

Padin, X. A., Vásquez-Rodríguez, M., Castaño, M., Velo, A., Alonso-Pérez, F. and co-authors. 2009. Air-sea $CO_2$ fluxes in the Atlantic as measured during the FICARAM cruises. *Biogeosci. Discuss.* **6**, 5589–5622.

Pierrot, D., Neill, C., Sullivan, K., Castle, R., Wanninkhof, R. and co-authors. 2009. Recommendations for autonomous underway $pCO_2$ measuring systems and data-reduction routines. *Deep-Sea Res.* **56**, 512–522.

Poisson, A., Metzl, N., Brunet, C., Schauer, B., Bres, B. and co-authors. 1993. Variability of sources and sinks in the western Indian and Southern oceans during the year 1991. *J. Geophys. Res.* **98**(C12), 22759–22778.

Richardson, P. L. and Reverdin, G. 1987. Seasonal cycle of velocity in the Atlantic North Equatorial Countercurrent as measured by surface drifters current meters and ship drift. *J. Geophys. Res.* **92**, 3691–3708.

Richey, J. E., Melack, J. M., Aufdenkampe, A. K., Ballester, V. M. and Hess, L. L. 2002. Outgassing from Amazonian rivers and wetlands as a large tropical source of atmospheric $CO_2$. *Nature* **416**, 617–620.

Seyler, P., Coynel, A., Moreira-Turcq, P., Etcheber, H., Colas, C. and co-authors. *Organic Carbon Transported by the Equatorial Rivers: Example of Zaire-Congo and Amazon Rivers* Advances in Soil Science Editions, Ohio, 2003.

Sweeney, C., Gloor, E., Jacobson, A. R., Key, R. M., McKinley, G. and co-authors. 2007. Constraining global air-sea gas exchange for $CO_2$ with recent bomb $^{14}C$ measurements. *Global Biogeochem. Cycles* **21**, doi:10.1029/2006GB002784.

Takahashi, T., Olafsson, J., Goddard, J. G. and Chipman, D. W. 1993. Seasonal variation of $CO_2$ and nutrients in the high-latitude surface oceans: a comparative study. *Global Biogeochem. Cycles* **7**(4), 843–878.

Takahashi, T., Sutherland, S. C., Wanninkhof, R., Sweeney, C., Feely, R. A. and co-authors. 2009. Climatological mean and decadal change in surface ocean $pCO_2$, and net sea-air $CO_2$ flux over the global oceans. *Deep-Sea Res.* **56**, doi:10.1016/j.dsr2.2008.12.009.

Ternon, J. F., Oudot, C., Dessier, A. and Diverres, D. 2000. A seasonal tropical sink for atmospheric $CO_2$ in the Atlantic ocean: the role of the Amazon River discharge. *Mar. Chem.* **68**(3), 183–201.

Wanninkhof, R. H. 1992. Relationship between wind speed and gas exchange over the ocean. *J. Geophys. Res.* **97**(C5), 7373–7382.

Weiss, R. F. 1974. $CO_2$ in water and seawater: the solubility of a non-ideal gas. *Mar. Chem.* **2**, 203–215.